Construction and Building Materials 79 (2015) 318–325

Contents lists available at ScienceDirect

Construction and Building Materials

journal homepage: www.elsevier.com/locate/conbuildmat

Strengthening of RC columns by longitudinal CFRP sheets: Effect of strengthening technique

Niloufar Moshiri *, Ardalan Hosseini, Davood Mostofinejad

Department of Civil Engineering, Isfahan University of Technology (IUT), Isfahan, Iran

HIGHLIGHTS

- Ten RC column specimens were strengthened with longitudinal CFRP sheets.
- Four different methods were used for strengthening of RC column specimens.
- Grooving method (GM) significantly increased the load capacity compared to EBR.
- PIV technique was used to investigate the bond behavior of CFRP-to-concrete under compression.
- PIV measurements verified that GM improves the bond of CFRP-to-concrete compared to EBR method.

ARTICLE INFO

Article history:
Received 24 July 2014
Received in revised form 25 December 2014
Accepted 4 January 2015
Available online 28 January 2015

Keywords:
RC column
CFRP
Buckling
Grooving method (GM)
Compressive strengthening
Particle image velocimetry (PIV)

ABSTRACT

In the present study, the effect of utilizing longitudinal carbon fiber reinforced polymer (CFRP), as external compression reinforcement, on the behavior of strengthened RC columns is investigated. To do so, 10 RC columns including 5 circular columns with diameter of 150 mm and 5 square columns with dimension of 133 mm were cast. Four different methods including conventional externally bonded reinforcement (EBR) and near surface mounted (NSM) techniques, as well as the recently introduced grooving method (GM) in the forms of externally bonded reinforcement on grooves (EBROG, to be pronounced as /ebrʌg/) and externally bonded reinforcement in grooves (EBRIG, to be pronounced as /ebrIg/) techniques were used to strengthen the specimens in compression with CFRP. The specimens were tested under monotonic uniaxial compression, and different effects of the strengthening techniques were comprehensively discussed. Furthermore, an image-based deformation measurement technique, i.e. particle image velocimetry (PIV) was used to further investigate the stress transfer between longitudinal CFRP sheet and concrete substrate. Experimental results demonstrated that utilizing grooving method (GM) for bonding CFRP to concrete surface postpones the CFRP buckling, and subsequently, a significant increase in load carrying capacity of strengthened RC columns by compression CFRP sheets was observed.

1. Introduction

The majority of experimental and numerical studies investigating the behavior of FRP-strengthened columns have been focused basically on columns confined with FRP hoop wraps; which results in a significant increase in load carrying capacity and ductility of the strengthened column. However, FRP composites with fibers aligned along or oblique to the column axis, as well as composites with multidirectional fibers can be also used for strengthening of columns [1]. Longitudinal composites, i.e. composites with fibers aligned along the column axis, contribute directly to load carrying capacity of column, through withstanding compressive stresses applied on the column [2].

Although some researchers state that FRP composites are able to tolerate compression, design and strengthening guidelines do not consider their compression strength [3–5]. A major reason may be the occurrence of global buckling of FRP under compression, in addition to other micromechanical failure modes [3]. However, considerable increase in load carrying capacity of columns strengthened with longitudinal FRP could be observed if the FRP sheets are effectively restrained by lateral supports; for instance, when they are confined by FRP hoop wraps [2]. Issa et al. [6] demonstrated that confining longitudinal CFRP with full-height wraps, results in significant increase in load carrying capacity of strengthened columns. Besides, they showed that using longitudinal CFRP as the external

* Corresponding author. Tel.: +98 31 3391 3818; fax: +98 31 3391 2700.
E-mail addresses: n.moshiri@cv.iut.ac.ir (N. Moshiri), a.hosseini@cv.iut.ac.ir (A. Hosseini), dmostofi@cc.iut.ac.ir (D. Mostofinejad).

http://dx.doi.org/10.1016/j.conbuildmat.2015.01.040
0950-0618/

layer over hoop wrap layer of FRP has no considerable influence on the behavior of the strengthened column. On the other hand, it was demonstrated by Fitzwilliam and Bisby that the strength capacity of slender CFRP reinforced columns can be increased by longitudinal CFRP [7].

Compression behavior of FRP composites is rarely investigated in the field of strengthening of columns with FRPs. In other words, longitudinal FRPs have not been widely used for external strengthening of RC columns subjected to concentric loading; while the existing literature on the issue investigated the simultaneous use of hoop wraps over longitudinal FRPs, and not pure effects of utilizing longitudinal FRPs [1,8]. In some other research works, concerning compressive behavior of FRP composites (see for example [9–11]), global buckling of FRP was prevented; and the compression strength of wet lay-up FRP used for strengthening of structural members was not investigated either. Therefore, it seems essential to study the compressive behavior of wet lay-up FRP used for external strengthening of structural members and introduce some techniques to improve its compression performance.

As it was mentioned before, one of the probable failure modes for the FRP composite under compression is its global buckling, which results in premature debonding of FRP from concrete substrate. In order to prevent debonding of tensile composite from concrete substrate in beams flexurally strengthened with FRP, grooving method (GM) has been introduced by Mostofinejad et al. [12–15] as a substitute for conventional EBR. Mostofinejad and Mahmoudabadi [12] introduced a technique of GM which was later named as externally bonded reinforcement on grooves (EBROG). They used this method to prevent debonding of tensile CFRP sheets from concrete substrate used for flexural strengthening of concrete beams [12]. Their experimental results showed that using GM increases the load capacity of the strengthened beams compared to EBR specimens and changes the failure mode of the specimens from debonding to rupture of CFRP sheets [12]. Mostofinejad and Tabatabaei [14] investigated the effect of GM on shear strengthening of beam specimens and reported the better performance of the specimens strengthened with FRP in shear using GM in the form of EBROG compared to those strengthened using EBR. In 2013, Mostofinejad and Shameli [13] presented another technique of GM called externally bonded reinforcement in grooves (EBRIG), in which the FRP sheets were in direct contact with the internal surfaces of the grooves on the tension face of a concrete beam in wet lay- up application. They demonstrated that the EBRIG technique results in higher load carrying capacity of strengthened specimens, especially when higher number of CFRP layers is used [13]. Experimental research works conducted by Hosseini and Mostofinejad [16,17] through single-shear tests, clearly demonstrated that utilizing EBROG technique significantly improves the bond behavior of CFRP-to-concrete. The results verified that interfacial bond characteristics (i.e. maximum interfacial shear stress and fracture energy) in EBROG joints are quite better than in conventional EBR [17].

Due to better transmission of interfacial shear stresses from FRP composite to concrete substrate in GM, in the current study, the method was utilized for bonding compression FRP to concrete columns. RC column specimens were strengthened with longitudinal CFRP sheets using different techniques including the grooving method as well as EBR and a special NSM method, as it is described in the next section. Effects of grooving method on the load carrying capacity of strengthened columns and postponing the buckling of CFRP sheets using wet lay-up procedure have been compared with EBR strengthened columns. Furthermore, a full field image-based deformation measurement technique, called particle image velocimetry (PIV) has been utilized to investigate the axial strain distribution in longitudinal CFRP sheets attached to concrete columns using EBR and EBROG techniques.

2. Experimental work

2.1. Test specimens and material properties

A total number of 10 reinforced concrete column specimens with height of 500 mm were constructed and tested under uniaxial compression. The test specimens were divided into two series (i.e. CC and SC) based on their cross section configuration. Series CC comprised of 5 columns with circular cross section of 150-mm diameter. Six deformed steel bars with 10-mm diameter were used as internal reinforcement providing a longitudinal steel ratio of 2.67%. Series SC included 5 columns with square cross section of 133-mm side dimension and 8 mm corner radius. The internal longitudinal steel ratio of these columns was 2.56% provided by four 12-mm diameter deformed bars. The transverse reinforcement in all specimens was comprised of 8-mm diameter stirrups spaced at 85 mm. Circular and square stirrups were used in specimens of series CC and SC, respectively. Clear concrete cover equal to 20 mm was provided over the steel reinforcements. Fig. 1 shows the reinforcement details. A concrete mix design was adopted to cast the RC column specimens with target 28-day compressive strength of 28 MPa. Compressive strengths of concrete were determined by testing 3 standard concrete cylinders (150×300 mm) for each series, simultaneous with column test.

The CFRP composite applied for strengthening of the specimens was prepared by carbon fiber sheets and epoxy matrix through wet lay-up procedure; which their mechanical properties, provided by the manufacturer, are presented in Table 1. The table also contains the mechanical properties of steel bars with different diameters.

The specimens details and test results are shown in Table 2. Each group of specimens included one control column specimen (designated as CC-Ref or SC-Ref) and four columns strengthened with longitudinal FRP using different bonding techniques. The specimens were labeled with their series name followed by the strengthening technique. These techniques included the conventional method of externally bonded reinforcements (EBR), two techniques of grooving method (EBROG & EBRIG) and a so-called near surface mounted (NSM) method; which are briefly explained in the following.

Eight carbon fiber sheets of 60 mm width and 390 mm length along the column axis were used for strengthening of column specimens in EBR, EBROG and EBRIG methods; and consequently the amount of FRP material in all strengthened columns was exactly the same. The surface preparation in EBR technique was performed through removing a thin layer of concrete by a grinding machine and cleaning with air jet; the fiber sheets were then bonded to concrete substrate through wet lay-up procedure. In EBROG and EBRIG techniques, 8 grooves with 10 mm depth, 10 mm width and 460 mm length along column axis, spaced at equal intervals across the column perimeter, were first cut in the column concrete cover and cleaned with air jet; without any conventional surface preparation on concrete surface. The clear distance between the grooves in circular specimens was nearly 49 mm. In square columns, 2 grooves were cut on each side of the specimen with clear distance of 55 between the grooves and 27 mm from the edge. In EBROG technique, the grooves were then filled with epoxy and fiber sheets were bonded onto the column surface. In EBRIG technique, the fiber sheets were directly bonded to concrete substrate being in direct contact with the internal surfaces of the groove as well as the exterior surfaces of the column perimeter (i.e. the intervals between the grooves). Then the grooves were filled with epoxy matrix. Detailed description of the GM is presented in [13,15].

In the NSM technique, utilized in the current study, 8 grooves with similar dimensions to those in EBROG and EBRIG techniques were first cut in the concrete cover and then, each of the eight

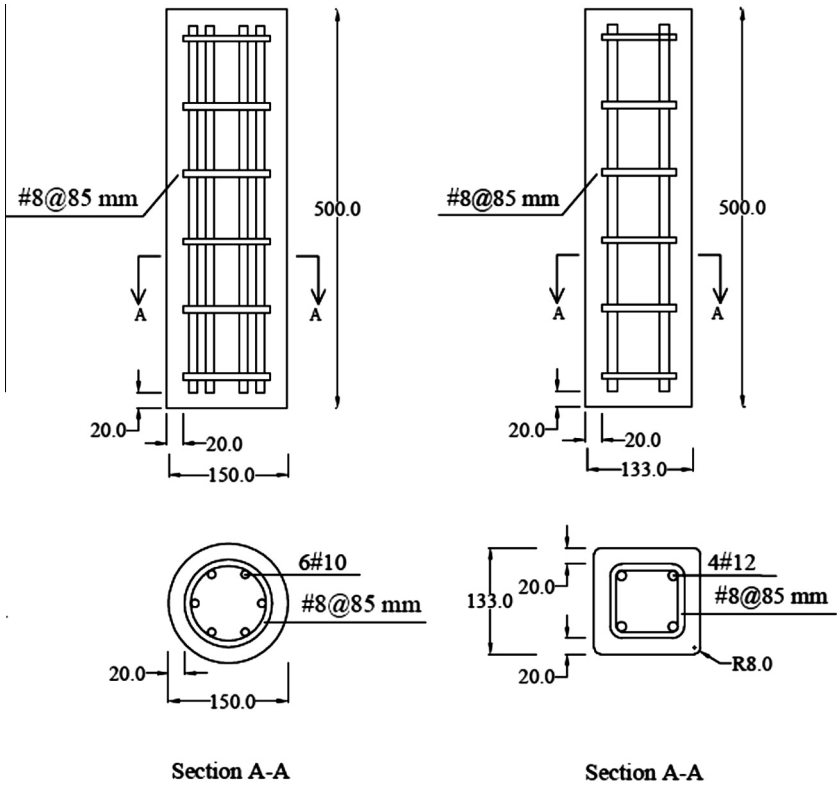

Fig. 1. Reinforcement details (all dimensions are in mm).

Table 1
Material properties.

(a) Steel	Diameter (mm)	Yield strength (MPa)	Ultimate strength (MPa)	
#8	8	550	774	
#10	10	406	538	
#12	12	340	515	
(b) Resin	Tensile strength (MPa)	Elastic modulus (GPa)	Ultimate tensile strain (%)	
Sikadur-330	30	4.5	0.9	
(c) Fiber	Tensile strength (MPa)	Elastic modulus (GPa)	Ultimate tensile strain (%)	Thickness (mm)
SikaWrap-230 C	4300	238	1.8	0.131

Table 2
Specimens details and summary of test results.

Series	Specimen	ε_a (%)	$\varepsilon_a/\varepsilon_{co}$	P_{max} (kN)	Increase in P_{max} (%)
CC	CC.Ref	1.1039	1.00	534.70	–
	CC.EBR	1.1438	1.04	548.69	2.6
	CC.EBROG	0.9920	0.90	610.11	14.1
	CC.EBRIG	0.9782	0.89	633.76	18.5
	CC.NSM	1.6555	1.50	550.66	3.0
SC	SC.Ref	1.2398	1.00	466.65	–
	SC.EBR	1.5988	1.29	462.19	−1.0
	SC.EBROG	–[a]	–[a]	515.28	10.4
	SC.EBRIG	1.3851	1.12	525.86	12.7
	SC.NSM	–[a]	–[a]	488.99	4.8

ε_a: axial strain at ultimate.
ε_{co}: axial strain of reference specimen at ultimate.
[a] Cannot be determined due to premature rupture of CFRP hoop wrap at one end of the column.

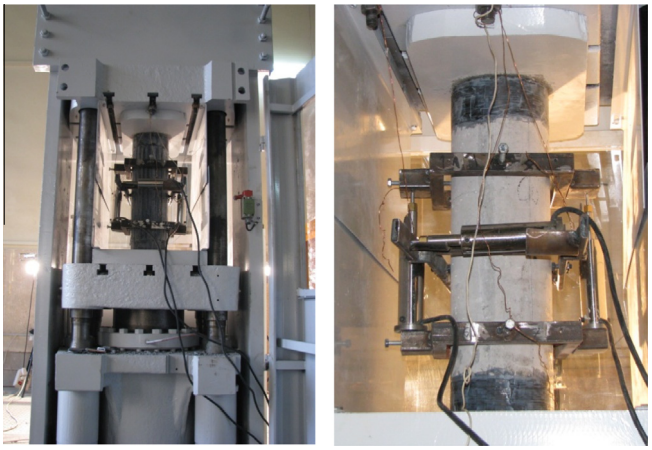

Fig. 2. Test setup and LVDTs.

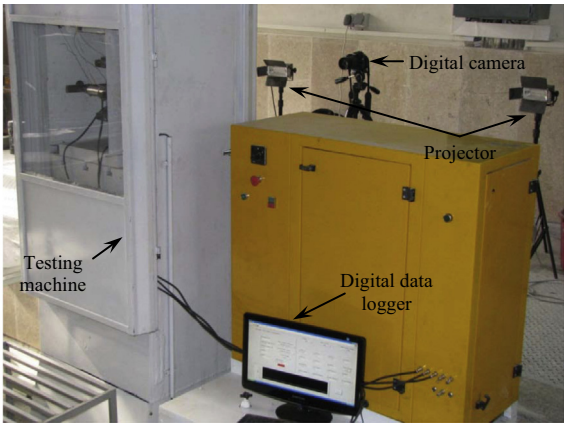

Fig. 3. Camera and projectors positions and testing machine.

60 × 390 mm fiber sheets similar to those used in the other three techniques was longitudinally divided into 8 narrower sheets and sequentially embedded in each groove. A thin coat of matrix was applied on each narrow sheet and the grooves were filled with epoxy matrix at the end. Therefore, a wet lay-up composite with the same amount of FRP as the other techniques, was produced in the NSM technique as well [13]. Note that although the amount of carbon fiber used in all the strengthening methods was exactly the same, however, the fiber volume fractions were slightly different in each strengthening technique due to the different amount of epoxy used. Finally, to avoid premature failure of the column ends which had no internal reinforcing (see Fig. 1), both ends of the column specimens were confined by one layer of CFRP wrap extending 55 mm from each end [18,19].

2.2. Instrumentation and testing

The specimens were subjected to unidirectional compressive loading using a testing machine of 2000 kN capacity. Load was applied on the columns by moving the below rigid support of the testing machine via a hydraulic jack with a constant rate of 1.0 mm/min, to be controlled by LVDTs used in the testing machine. As it is illustrated in Fig. 2, axial deformations of the column specimens were measured by using two LVDTs at the mid-height of the specimen. The two LVDTs with a gauge length of 20 mm and a resolution of 0.005 mm were mounted 180° apart on circular columns or on two opposite sides of columns with square sections. Axial strains were reported as the average recordings of the LVDTs divided by the primary gauge length of 240 mm. Radial deformations of columns were measured by using a horizontal LVDT same as the other two. Radial strains were determined by dividing the measurements of the horizontal LVDT by the column diameter or side dimension for circular and square columns, respectively. The test setup as well as the utilized LVDTs is presented in Fig. 2. It is worth mentioning that the vertical LVDTs mounting system was held tightly to the column surface which is covered by FRP sheets in strengthened specimens. However, the screws may be inserted in the concrete cover slightly. The horizontal LVDT mounting system was held on the column surface to an extent that it would not be dropped down.

2.3. Deformation measurement using particle image velocimetry (PIV)

In addition to the conventional deformation measurement technique, i.e. utilizing LVDTs, an image-based deformation measurement technique called particle image velocimetry (PIV) was used to monitor full field deformations of the tested columns during the loading process. PIV is originally a velocity-measuring technique which was first developed by Adrian [20] in the field of experimental fluid mechanics. A modified approach was used to implement PIV in geotechnical testing by White et al. [21]. Accurate full field deformation measurements can be obtained from the technique by analyzing successive digital images taken from a field undergoing deformation [17]. Since detailed review on the PIV method is beyond the scope of the current paper, the readers are referred to White et al. [21] for further information including detailed procedure, source of errors and precision validation experiments. Moreover, capability of the technique to accurately investigate FRP-to-concrete bond behavior has been comprehensively discussed by the authors in [16,17,22].

In the current study, one CCD (charge couple device) digital camera, i.e. Nikon D80 with resolution of 10.0 megapixels (3872 × 2592 pixels) having a Nikkor 18–135 mm lens was placed perpendicular to the specimens face at a distance equal to 1.0 m. Digital images were automatically taken from each specimen undergoing deformation using a remote control at regular intervals. It is necessary for the images to have a proper texture to create features upon which image processing can operate [16,17,22]. Since CFRP sheets originally does not show suitable texture, natural colored sand between sieve Nos. 50 and 100, obtained from mixing equal proportions of five different colors, was embedded to all specimens faces at the end of the wet lay-up procedure and before epoxy hardening. Obviously, embedded sand has no any effects on the response and behavior of the specimens [22]. A digital data logger was used to monitor the load cell, LVDTs and image numbers, simultaneously. Moreover, the specimens were illuminated using two white light projectors to eliminate any probable parasitic lights. Camera and projectors positions and the testing machine are presented in Fig. 3. After performing the tests, all the captured images were analyzed using GeoPIV8 software, developed at Cambridge University [23].

3. Results and discussion

Tests results and the load–strain curves of column specimens are presented in Table 2 and Fig. 4, respectively. P_{max} and ε_a in Table 2 are the maximum load and ultimate axial strain of column specimens, respectively; and ε_{co} is the ultimate axial strain of reference unstrengthened column in each group. As it is observed in Fig. 4, there was no distinctive failure point on the load–strain curves of specimens; subsequently, load level equal to 85% of the maximum load on descending branch was defined as the ultimate point of load–strain curves, where ε_a in Table 2 was determined at.

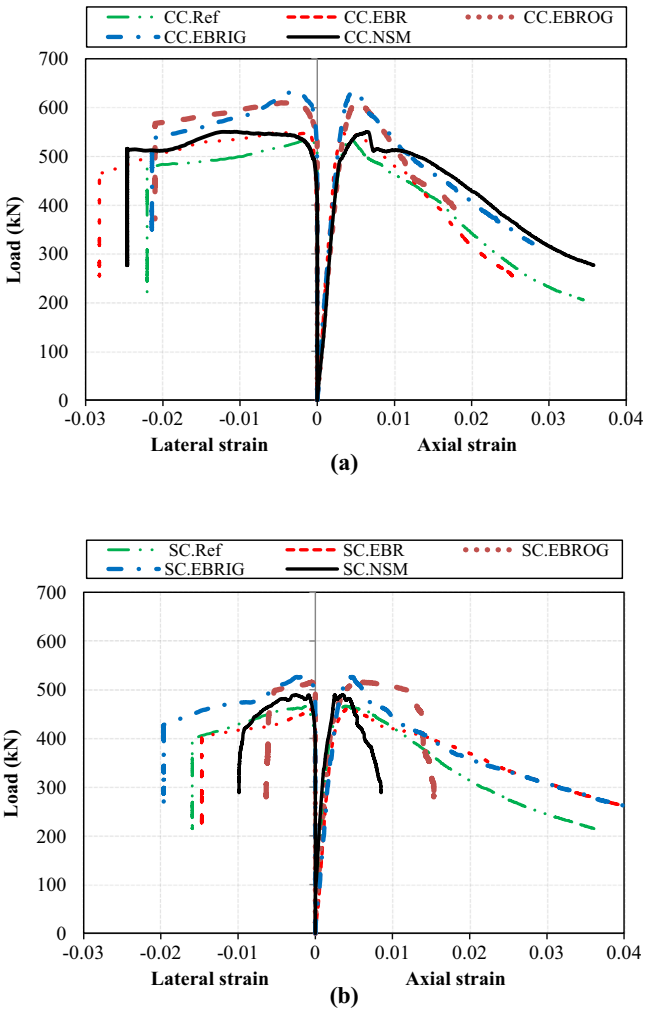

Fig. 4. Load–strain curves of tested columns; (a) series CC, (b) series SC.

3.1. Load carrying capacity

3.1.1. Columns with circular section (series CC)

Comparing the load and strain characteristics of the strengthened columns with those of the reference one (Fig. 4(a) and Table 2), shows that a considerable increase in load carrying capacity was obtained when grooving method was used. Specimens "CC.EBROG" and "CC.EBRIG" had maximum loads of 610.1 kN and 633.8 kN, respectively, indicating 14.1% and 18.5% increase over the control column, having a maximum load bearing capacity of 534.7 kN. On the other hand, specimen "CC.EBR" showed little increase respect to control column by tolerating 548.7 kN (indicating 2.6% increase compared to the control column). When a column is strengthened with longitudinal FRP, compressive stresses applied on the column would be transferred to the FRP composite through its bond to concrete substrate. Therefore, the composite is confronted with compression which may lead to its buckling and debonding from column substrate. It seems that the longitudinal grooves in GM, provide lateral supports to postpone FRP buckling and thus increase the load capacity of specimens. Furthermore, EBRIG technique was more efficient in increasing the load carrying capacity of specimens due to direct contact between FRP and concrete substrate. It is seen in Table 2 that utilizing the special NSM method for strengthening the RC column did not significantly increase the load capacity of the specimens; which may be attributed to the application of wet lay-up composite through compacted fiber sheets in grooves. Further explanations are given in the next part where specimen "SC.NSM" is described.

3.1.2. Columns with square section (series SC)

Similar to the results of series CC, Table 2 reveals significant improvement in maximum loads of columns strengthened with EBROG and EBRIG techniques in series SC. It can be seen in this table that 10.4% and 12.7% increase in load capacity, compared to the control column, was observed in specimens "SC.EBROG" and "SC.EBRIG", respectively. Whereas, specimen "SC.EBR" carried a maximum load almost equal to that of control specimen. Trend of maximum load enhancements for different techniques in series SC was identical to those of series CC, confirming the results. It should be noted that each fiber sheet tends to buckle separately from other sheets; because there was no overlap between the sheets. Therefore, the moment of inertia of each sheet measured to its centroid (and not the centroid of the column section) was effective on the critical load of buckling. Although the cross section of each CFRP strip in the horizontal plane was a thin rectangle for columns of group SC, it was a curved section for columns of group CC; leading to higher moment of inertia of each CFRP strip respect to the centroid of the strip. Therefore, buckling of composite in circular strengthened columns would occur later compared to square columns, and therefore, load capacity of circular columns improves further.

It is shown in Table 2 that the maximum load of specimen "SC.NSM" was equal to 489.0 kN, indicating 4.8% increase compared to the control column. Moreover, it can be seen in Table 2 that specimen "CC.NSM" carried a maximum load of 550.7 kN indicating 3.0% increase in load capacity compared to the reference circular specimen. Though such increase is not so significant, some reasons may be attributed to better performance of NSM method in square column specimen compared to that in the circular one. By cutting a groove with a grinding machine in the circular column, surfaces of the groove would not be so smooth due to the machine setup and its incompatibility with curvature of the column. Therefore, it would cause some damage, scratches or fiber misalignments in the composite. This phenomenon would diminish the compression performance of the whole composite in NSM method, since the entire fiber sheets are concentrated in grooves. In other words, the labor work resulted in a rough substrate. Since the compressive FRP is very sensitive to misalignments, the aforementioned fact decreases the FRP performance. Therefore, weaker performance would be expected when NSM method is used in circular columns compared to square specimens (in which the surfaces are more smooth and even). Note that the mentioned phenomenon does not affect the whole composite in EBRIG method; because not all the fiber sheets are bonded in the grooves in EBRIG, and thus, this method can perform appropriately.

3.2. Overall behavior of column specimens

It is observed during the tests that in strengthened specimens, buckling and debonding of longitudinal FRP from concrete substrate occurred before reaching the maximum load and continued gradually as the applied load increased. When the load further increased, more parts of the CFRP sheets buckled and their protrusions further developed. This process resulted in a gradual and not abrupt failure of the strengthened columns. Figs. 5 and 6 show the failure styles of the specimens in series CC and SC, respectively.

It is seen in Fig. 6 that in specimens "SC.EBROG" and "SC.NSM", one of the ending hoop wraps ruptured during the loading. Since it happened after reaching the peak load of the column, it can be concluded that the maximum load reported for these column specimens are trustworthy. However, the premature rupture of hoop wrap affected the columns behavior; i.e. no large protrusions were

CC.Ref CC.EBR CC.EBROG CC.EBRIG CC.NSM

Fig. 5. Failure modes of columns in series CC.

SC.Ref SC.EBR SC.EBROG SC.EBRIG SC.NSM

Fig. 6. Failure modes of columns in series SC.

observed in mid-height of the columns. In other words, due to the rupture of hoop wraps, larger deformations occurred at that end and axial strains of mid-height of the column were observed to be smaller compared to other specimens. This fact resulted in obtaining an inaccurate load–strain curve after the maximum load (see Section 3.3 and Fig. 4(b)). Therefore, the ultimate axial strains (ε_a) for these two specimens were not reported in Table 2.

3.3. Stress–strain behavior

Fig. 4 shows the load–strain curves for all the specimens of series CC and SC, based on the strain values obtained from LVDTs. The load–axial strain curve of each specimen is comprised of an ascending branch followed by a descending one in which, the carried load of the column decreases gradually (without a major reduction in load) accompanied with increasing of axial strains. It leads to the fact that the failure mode of column specimens was gradual and not abrupt, as it was mentioned before. It is worth mentioning that the loading procedure was continued as far as the instrumentations worked properly and the load–strain curves of the specimens were recorded up to this point.

It can be observed in Fig. 4 that the load–strain behavior of FRP-strengthened columns are similar to control ones (except specimens "SC.EBROG" and "SC.NSM"); i.e. the slope of curves are almost identical either before or after the maximum load, showing the fact that longitudinal FRP did not considerably affect the stiffness of the strengthened RC columns. It is demonstrated in Fig. 4(b) that descending branches of load-axial strain curves of specimens "SC.EBROG" and "SC.NSM" do not properly match the curves of other specimens in this group, which is due to the premature rupture of CFRP hoop wrap at one end of the column, as it was mentioned earlier.

3.4. PIV measurements

3.4.1. Validation of the technique

Capability of PIV in accurate deformation measurements has been demonstrated by White et al. [21]. Furthermore, application of the technique as an alternative to conventional foil strain gauges to measure strain localization in FRP-confined concrete was comprehensively discussed and validated in [24,25]. Hosseini et al. [26,27] also conducted extensive validation experiments to show the great potential of the technique in accurate displacement and strain fields measurements in structural tests. Consequently, there is no doubt regarding the accuracy of the PIV results; however, a comparison between LVDT and PIV measurements, in term of strain, is indicatively demonstrated here.

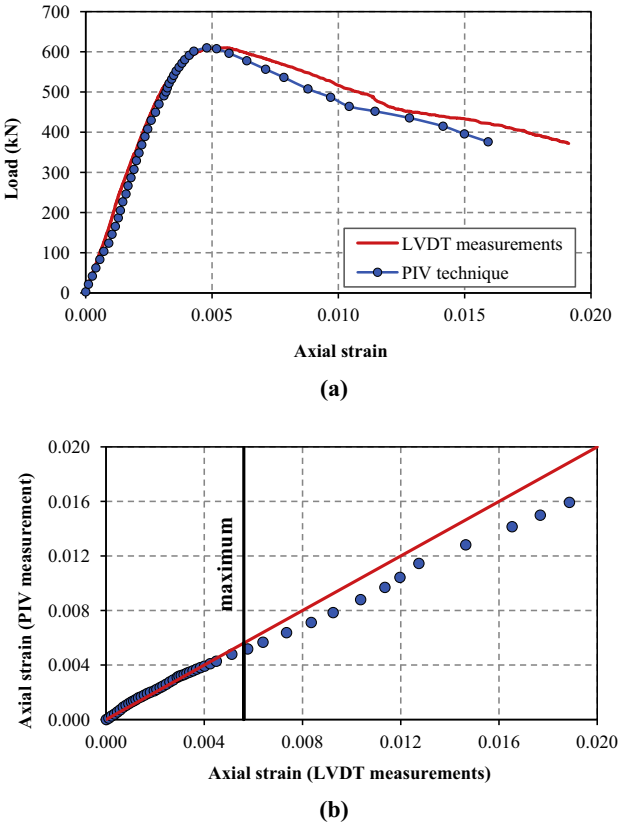

Fig. 7. Comparison of strains obtained by PIV technique and LVDTs measurements for specimen "CC.EBROG"; (a) load–axial strain curve, (b) comparison of axial strains in two methods.

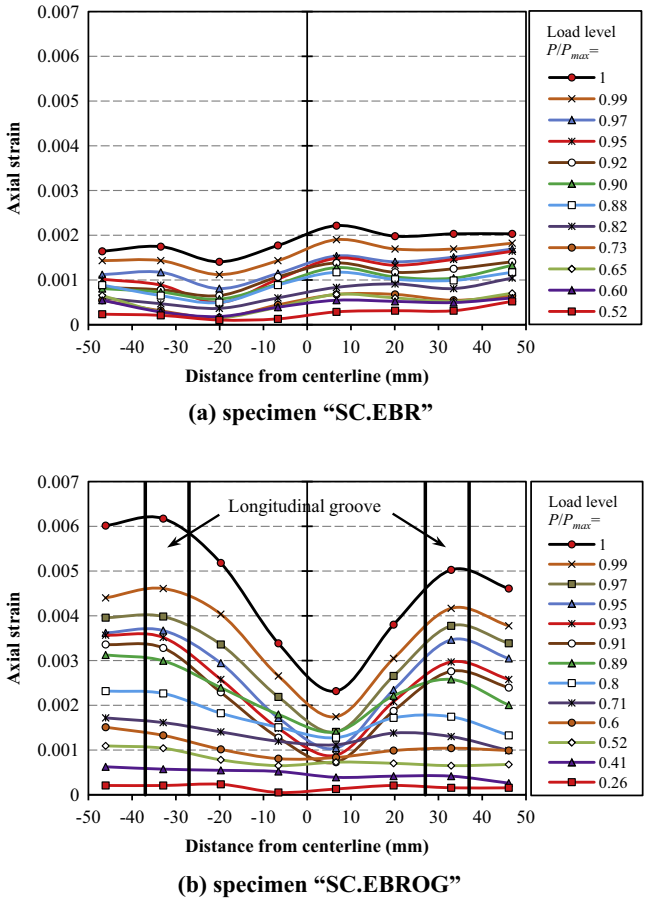

Fig. 8. Evolution of axial strain profile along width of column during loading; (a) specimen "SC.EBR" (P_{max} = 462.19 kN); (b) specimen "SC.EBROG" (P_{max} = 515.28 kN).

Fig. 7 shows typical results of the validation study, performed as part of the current paper, for specimen "CC.EBROG" by presenting a comparison of axial strain measured using LVDT and PIV. PIV measurements were performed using *virtual strain gauges*, made up of two 128 × 128 pixel patches. A more detailed explanation of the strain measurements utilizing virtual strain gauges can be found in [26]. In order to perform a realistic comparison between LVDT readings and PIV measurements, the length of the generated virtual strain gauges were considered to be the same as LVDTs' (approximately equal to 240 mm). In general, the agreement between load–strain responses obtained from LVDT and PIV is excellent, especially up to the maximum load level. As it is shown in Fig. 7(b), the correlation between axial strains obtained from PIV and LVDT is great up to the maximum load level, since an average discrepancy of 0.0029 percent, which is equal to 29 microstrains, was observed between strain values obtained from LVDT and PIV. However, after reaching the maximum load level, LVDTs recorded larger strain values compared to PIV measurements, which can be attributed to the fact that the PIV results can be seriously affected by buckling of the longitudinal FRP composite, developed almost after reaching the maximum load level; while this issue may not affect the LVDT readings, due to the utilized special frame shown in Fig. 2.

3.4.2. Axial strain profiles along width of the columns

Since the PIV technique provides accurate strain data, it is instructive to use the technique to investigate the variation in axial strain profile along the perimeter of the columns; this has been performed in Fig. 8(a) and (b), respectively for specimens "SC.EBR" and "SC.EBROG" strengthened by EBR and EBROG techniques. To obtain the axial strain profiles, 8 virtual strain gauges were generated along the width of the specimens, at the mid-height, through PIV procedure. It is noteworthy that the length of the utilized virtual strain gauges was approximately equal to 27 mm; each consisted of two 128 × 128 pixel patches.

As it is presented in Fig. 8(a), the axial strain distribution in longitudinal CFRP attached to concrete using EBR method was more or less uniform along the width of the column; while the strain profiles gradually increased by load increase, up to the maximum load. It should be noted here that, axial strain distribution in the CFRP sheet along the width of the column is not expected to be exactly uniform due to intrinsic local differences in the bond, as well as the workmanship in wet lay-up applications [16]. Axial strain distribution in specimen "SC.EBROG" was almost the same as in specimen "SC.EBR" up to 0.7 P_{max} (Fig. 8(b)). In other words, the strain profiles gradually increased by increase of load up to 0.7 P_{max}. However, beyond this load level, the CFRP sheets, attached on the grooves, reached comparatively higher strain values up to the maximum load level (P_{max}); since stronger bond between FRP composite and concrete substrate could be reached through the epoxy-filled grooves, which has been comprehensively discussed by Hosseini and Mostofinejad in [16]. Thus, the CFRP sheets attached on the grooves had proper lateral support which prevented from buckling. Furthermore, careful inspection of Fig. 8(b) reveals that by increasing the load level from 0.89 P_{max} to 0.91 P_{max}, strain in the CFRP sheets attached between the longitudinal grooves, suddenly released. The reason can be attributed to the buckling and the subsequent debonding of the CFRP sheets in this zone. It may be noted here that the main intention of the current

study is to show the capability of GM (in the forms of EBROG and EBRIG techniques) in utilization of compression capacity of FRP composites, when used for external strengthening of RC columns. Hence, extra studies are definitely needed to further investigate the effect of groove characteristics on FRP-to-concrete bond behavior of EBROG (EBRIG) joints under compression loading.

4. Conclusions

This paper studied the effect of strengthening techniques on the load carrying capacity of column specimens externally strengthened with longitudinal composites. Based on the experimental results and PIV measurements, the following conclusions can be drawn.

1. Experimental results indicated that utilizing the grooving method for compression strengthening of RC columns with longitudinal CFRP resulted in considerable increase in load carrying capacity of the column; while conventional EBR method did not noticeably improve the column maximum load. For instance, maximum loads of circular columns strengthened with EBROG and EBRIG techniques were increased 14.1% and 18.5% compared to reference column; while this increase value was 2.6% for the column strengthened with EBR.
2. It was observed that the EBRIG technique is more efficient than EBROG in improving the load carrying capacity of the strengthened column; although, the complexity of EBRIG in practice would increase the labor cost.
3. Tests results revealed that utilizing the grooving method, postpones the buckling and debonding of compression CFRP from concrete substrate due to providing a proper lateral support for the composite; which is in fact, the main reason of successful performance of GM in compression strengthening of RC columns with longitudinal FRPs. On the other hand, the EBR method was not so efficient in utilization of compressive capacity of longitudinal composite.
4. Due to the flat surfaces of columns with square sections, their maximum loads enhancements were smaller compared to columns with circular cross sections; i.e. the increase in load capacity in specimen "SC.EBROG" was observed as 10.4%; while it was 14.1% in specimen "CC.EBROG".
5. Evolution of the axial strain profile in the CFRP sheets along the width of the columns obtained from PIV measurements, demonstrated the capability of the GM to provide much stronger bond between FRP composite and concrete substrate, compared with conventional EBR method. This behavior leads to satisfactory utilization of the compression capacity of FRPs under compression loading.

References

[1] Piekarczyk J, Piekarczyk W, Blazewicz S. Compression strength of concrete cylinders reinforced with carbon fiber laminate. Constr Build Mater 2011; 25(5):2365–9.

[2] Tan K. Strength enhancement of rectangular reinforced concrete columns using fiber-reinforced polymer. J Compos Constr ASCE 2002;6(3):175–83.

[3] ACI Committee 440.2R. Guide for the design and construction of externally bonded FRP systems for strengthening concrete structures. ACI 440.2R-08. Farmington Hills, MI, USA; 2008.

[4] JSCE. Recommendations for upgrading of concrete structures with use of continuous fiber sheets. Concrete Engineering Series; vol. 41; 2001.

[5] Technical Report No. 55. Design guidance for strengthening concrete structures using fiber composite materials. UK: The Concrete Society; 2004.

[6] Issa M, Alrousan R, Issa M. Experimental and parametric study of circular short columns confined with CFRP composites. J Compos Constr ASCE 2009;13(2): 135–47.

[7] Fitzwilliam J, Bisby L. Slenderness effects on circular CFRP confined reinforced concrete columns. J Compos Constr ASCE 2010;14(3):280–8.

[8] Au C, Buyukozturk O. Effect of fiber orientation and ply mix on fiber reinforced polymer-confined concrete. J Compos Constr ASCE 2005;9(5): 397–407.

[9] Wilczynski AP. Longitudinal compressive strength of a unidirectional fibrous composite. Compos Sci Technol 1992;45(1):37–41.

[10] Yokozeki T, Ogasawara T, Ishikawa T. Nonlinear behavior and compressive strength of unidirectional and multidirectional carbon fiber composite laminates. Composites Part A 2006;37(11):2069–79.

[11] Lee J, Soutis C. A study on the compressive strength of thick carbon fibre–epoxy laminates. Compos Sci Technol 2007;67(10):2015–26.

[12] Mostofinejad D, Mahmoudabadi E. Grooving as alternative method of surface preparation to postpone debonding of FRP laminates in concrete beams. J Compos Constr ASCE 2010;14(6):804–11.

[13] Mostofinejad D, Shameli SM. Externally bonded reinforcement in grooves (EBRIG) technique to postpone debonding of FRP sheets in strengthened concrete beams. Constr Build Mater 2013;38:751–8.

[14] Mostofinejad D, Tabatabaei Kashani A. Experimental study on effect of EBR and EBROG methods on debonding of FRP sheets used for shear strengthening of RC beams. Composites Part B Eng 2013;45(1):1704–13.

[15] Mostofinejad D, Shameli SM, Hosseini A. EBROG and EBRIG methods for strengthening of RC beams by FRP sheets. Eur J Environ Civ Eng 2014;18(6): 652–68.

[16] Hosseini A, Mostofinejad D. Experimental investigation into bond behavior of CFRP sheets attached to concrete using EBR and EBROG techniques. Composites Part B Eng 2013;51:130–9.

[17] Hosseini A, Mostofinejad D. Effect of groove characteristics on CFRP-to-concrete bond behavior of EBROG joints: experimental study using particle image velocimetry (PIV). Constr Build Mater 2013;49:364–73.

[18] Gibbons ME. Behavior of corroded reinforced concrete columns with carbon fiber reinforced polymer jackets and columns with internal glass fiber reinforced polymer spirals: The University of Utah, Department of Civil and Environmental Engineering; 2011.

[19] Wang Z, Wang D, Smith S, Lu D. CFRP-confined square RC columns. I: Experimental investigation. J Compos Constr ASCE 2011;16(2):150–60.

[20] Adrian RJ. Particle imaging techniques for experimental fluid mechanics. Ann Rev Fluid Mech 1991;23:261–304.

[21] White DJ, Take WA, Bolton MD. Soil deformation measurement using particle image velocimetry (PIV) and photogrammetry. Geotechnique 2003;53(7):619–31.

[22] Hosseini A, Mostofinejad D. Effective bond length of FRP-to-concrete adhesively-bonded joints: experimental evaluation of existing models. Int J Adhes Adhes 2014;48:150–8.

[23] White DJ, Take WA. GeoPIV: Particle Image Velocimetry (PIV) software for use in geotechnical testing. Cambridge University, Engineering Department: Technical Report, D-SOILS-TR322; 2002.

[24] Bisby LA, Take WA, Caspary A. Quantifying strain variation in FRP confined concrete using digital image correlation: proof-of-concept and initial results. In: Smith ST, editor. Proc Asia-Pacific conf on FRP in structures, APFIS, Hong Kong, China; 2007. p. 599–604.

[25] Bisby LA, Take WA. Strain localization in FRP-confined concrete: new insights. Proc ICE Struct Build 2009;162(5):301–9.

[26] Hosseini A, Mostofinejad D, Hajialilue-Bonab M. Displacement and strain field measurements in steel and RC beams using particle image velocimetry. Eng Mech ASCE 2014;140(11). http://dx.doi.org/10.1061/(ASCE)EM.1943-7889.0000805.

[27] Hosseini A, Mostofinejad D, Hajialilue-Bonab M. Displacement measurement of bending tests using digital image analysis method. Int J Eng Tech 2012; 4(5):642–4.